FEB - FRESENIUS ENVIRONMENTAL BULLETIN
Founded jointly by F. Korte and F. Coulston
Production by PSP - Vimy Str. 1e, 85354 Freising, Germany in cooperation with PRT-Parlar Research & Technology
Vimy Str 1e, 85354 Freising
Copyright© by PSP and PRT, Vimy Str. 1e, 85354 Freising, Germany
All rights are reserved, especially the right to translate into foreign language or other processes - or convert to a machine language, especially for data processing equipment - without written permission of the publisher. The rights of reproduction by lecture, radio and television transmission, magnetic sound recording or similar means are also reserved.
Printed in Germany-ISSN 1018-4619

FEB-EDITORIAL BOARD

CHIEF EDITOR:
Prof. Dr. H. Parlar
Parlar Research & Technology-PRT
Vimy Str.1e
85354 Freising, Germany

MANAGING EDITOR:
Dr. P. Parlar
Parlar Research & Technology
PRT, Vimy Str.1e
85354 Freising, Germany

CO-EDITORS:

Environmental Spectroscopy
Prof. Dr. A. Piccolo
Universita di Napoli "Frederico II"
Dipto. Di Scienze Chemica Agrarie
Via Universita 100, 80055 Portici, Italy

Environmental Biology
Prof. Dr. G. Schuurmann
UFZ-Umweltzentrum
Sektion Chemische Ökotoxikologie
Leipzig-Halle GmbH,
Permoserstr.15, 04318
04318 Leipzig, Germany
Prof. Dr. I. Holoubek
Recetox-Tocoen
Kamenice126/3, 62500 Brno, Czech Republic
Prof. Dr. M. Hakki Alma
Igdir Universitesi
76000, Igdir, Turkey
Prof. Dr. A. Reichlmayr-Lais
Technical University of Munich
Arcisstraße 31
80333 Muenchen,Germany

Environmental Management
Dr. K. I. Nikolaou
Env.Protection of Thessaloniki
OMPEPT-54636 Thessaloniki
Greece

Environmental Toxicology
Prof. Dr. H. Greim
Senatkommision – DFG / TUM
85350 Freising, Germany

Environmental Proteomic
Dr. A. Fanous
Halal Control GmbH
Stahlstraße 44
D-65428 Rüsselsheim, Germany

Environmental Analytical Chemistry
Prof. Dr. M. Bahadir
Lehrstuhl für Ökologische Chemie
und Umweltanalytik
TU Braunschweig
Lehrstuhl für Ökologische Chemie
Hagenring 30, 38106 Braunschweig, Germany
Dr. D. Kotzias
Via Germania29
21027 Barza(Va), Italy
Prof. Dr. R. Kallenborn
Norwegian University of Life Sciences
Universitetstunet 3
1430 As,Norway

Environmental Education
Prof. Dr. C. Bayat
Yeni Yüzyil Üniversitesi
34010 Zeytinburnu, Istanbul, Turkey

Environmental Medicine
Prof. Dr. I. Tumen
Bandirma 17 Eylül Üniversitesi
10200 Bandirma, Turkey
Dr. J. Burhenne
Universitaet Klinikum
Im Neuenheim Feld 410
69120 Heidelberg,Germany

Advisory Board
K. Bester, K. Fischer, DCG. Muir,
R. Niessner,W.Vetter, D. Steinberg,
J. P. Lay, L. O. Ruzo

Marketing Manager
Cansu Ekici, MSC. of B.A.
PRT-Research and Technology
Vimy Str 1e
85354 Freising, Germany
E-Mail: parlar@wzw.tum.de
parlar@prt-parlar.de
Phone: +49/8161887988

Fresenius Environmental Bulletin is abstracted/indexed in:
Biology & Environmental Sciences, BIOSIS, CAB International, Cambridge Scientific abstracts, Chemical Abstracts, Current Awareness, Current Contents/Agriculture, CSA Civil Engineering Abstracts, CSA Mechanical & Transportation Engineering, IBIDS database, Information Ventures, NISC, Research Alert, Science Citation Index (SCI), Scisearch, Selected Water Resources Abstracts

CONTENTS

ERRATUM

© by PSP Volume 31– No. 01A/2022 pages 940-953 Fresenius Environmental Bulletin

SPATIAL AND TEMPORAL VARIABILITY OF TYPICAL AIR POLLUTANT CONCENTRATIONS IN THE URBAN AREA OF QINGDAO, CHINA

Xun Zhang[1], Bin Zhang[1], Yuchai Wan[1], Yanling Xu[2], Xiansheng Liu[3,4,*]

[1]Beijing Key Laboratory of Big Data Technology for Food Safety, School of Computer and Information Engineering, Beijing Technology and Business University, Beijing 100048, China
[2]College of Plant Health and Medicine, Qingdao Agricultural University, Qingdao, 266109, China
[3]Joint Mass Spectrometry Center, Cooperation Group Comprehensive Molecular Analytics, Helmholtz Zentrum Munchen, German Research Center for Environmental Health, Ingolstädter Landstr. 1, 85764 Neuherberg, Germany
[4]Joint Mass Spectrometry Center, Chair of Analytical Chemistry, University of Rostock, Rostock, 18059, Germany

ABSTRACT

Atmospheric pollutants have become a serious concern to the Chinese public in recent years due to the reduction of visibility and severe health risks associated with them. In this study, $PM_{2.5}$, PM_{10}, NO_2, and SO_2 were measured at a time resolution of 1-hour over the course of a year from January to December 2015 in the urban environment of Qingdao based on the temporal and spatial variations in the concentrations of four air pollutants. We found that (1) seasonal variation exists consistently for all pollutants, with the highest concentration in winter and the lowest in summer. (2) The monthly average of the concentrations of the four air pollutants exhibited U-shaped pattern of "high in autumn and winter but low in spring and summer", and the double-peak or single-peak impulse-shaped daily variation. $PM_{2.5}$ and PM_{10} concentrations were lower on weekdays than on weekends while SO_2 concentrations were higher on weekdays than on weekends, indicating a "weekend effect". (3) $PM_{2.5}$, PM_{10}, NO_2, and SO_2 factors showed strong correlation and low coefficient of divergence (CD) values at nine sites throughout the year, indicating an even distribution across the urban area. (4) Spatial autocorrelation analysis was used to characterize spatial variability showing that air pollutants in urban areas are not produced in the specific local site. The spatial distribution of annual and seasonal air pollution concentrations simulated by ordinary kriging showed that most parts of urban Qingdao suffer from severe air pollution in winter and pollutant concentrations are higher inland than at coastal sites.

KEYWORDS:
Air pollution, atmospheric pollutant concentrations, spatial-temporal characteristics, monitoring data, Qingdao urban area

INTRODUCTION

Urban areas with a high concentration of people and anthropogenic industrial and transport activities exhibit both the highest pollution levels and the largest targets of impact [1] . Urban and regional epidemiological studies have founda significant correlation between particulate matter (PM) exposure and mortality from cardiopulmonary and lung cancers, especially fine particulate matter and sulfur oxide–related pollution [2-5]. In addition, WHO (2012) [6] has reported that chronic exposure to air pollutants, including particulate matter (PM), causes the death of 7 million people, making it the world's most important environmental health risk.

Fine particles ($PM_{2.5}$ particles smaller than 2.5 μm in diameter) and coarse particles ($PM_{10-2.5}$— smaller than 10 μm in diameter but larger than 2.5 μm, CPM) are defined as amodal structure of particle size distributions typically observed in the atmosphere [2]. Fine particles and coarse particles are to be considered as separate classes of pollutants. These two PM size fractions are covered in PM_{10} (particles smaller than 10 μm in diameter) and can have substantially different sources and sinks [7]. Therefore, the PM source can be analyzed by the ratio of $PM_{2.5}$ and PM_{10}. It is well known that the fine particles originate mainly from combustion processes and gas-to-particle (SO_2, NO_2, HC et al.) conversion processes in the atmosphere. Therefore, in terms of mass concentration, the higher $PM_{2.5}/PM_{10}$, the higher the contribution rate of the secondary particles; the lower the ratio, the higher the contribution rate of the dust source. Other studies have shown that urban NO_2 mainly originates from mobile pollution sources such as automotive exhaust emissions, while SO_2 mainly originates from fixed sources such as industrial combustion (coal-fired power generation, metal smelting, etc.) [8]. Therefore, the higher the NO_2/SO_2 ratio, the higher the contribution of mobile pollution sources. The lower the ratio, the higher the contribution rate of fixed pollution sources.

Based on these knowledge, the objective of this study are: 1) to show the spatial-temporal characteristics of aerosols in urban cities by combining four indicators of atmospheric pollutants; 2) to explore the trend of atmospheric pollutants in workday and weekend; 3) and to portray the present situation of four indicators of atmospheric pollutants using geospatial statistical tools systematically. These estimates may be useful in assessing health impacts through related studies and in communicating with the public and policy makers for potential intervention.

MATERIALS AND METHODS

Data collection. In this manuscript, the urban area throughout Qingdao has been used as the study area. $PM_{2.5}$, PM_{10}, NO_2, and SO_2 concentrations data derived from urban air quality monitoring data of China's National Environmental Monitoring Centre [9]. The observation includes hourly pollutant concentrations at nine monitoring sites in Qingdao in 2015 to characterize the spatial variability of particulate matter concentrations (Figure 1). The detailed description of the monitoring sites is listed in Table 1.

Data preparation. According to Ambient Air Quality Standards (AAQS) of China GB3095-2012 , requirements for the validity of air pollutants concentration data, the data quality control, were conducted. The missing values and the outliers of $PM_{2.5}$, PM_{10}, NO_2, and SO_2 concentrations in the raw data were excluded using the Bayesian method, which is an important technique in statistics. In addition, the "daily average" refers to the arithmetic mean of the average daily 24-hour concentration; the "monthly average" refers to the arithmetic mean of the daily average concentration in a month; the "seasonal average" refers to the arithmetic mean of the average daily concentration in the calendar quarter; the "annual average" refers to the arithmetic mean of the average daily concentration in the calendar year.

Statistical analysis. Partial Correlation Analysis. The correlation between the concentrations of the two atmospheric pollutants can reflect the characteristics of the origin. When there is a positive correlation, this indicates that the two may have homology; when there is a negative correlation, the concentration of the two has a change characteristic. One may be the precursor of the other, at which point the secondary pollutant generation process is accelerated [10-12]. Therefore, the correlation analysis with Bivariate Correlations Analysis was completed using the Statistical Package of the Social Sciences 18.0 (SPSS 18.0) Software for Windows.

FIGURE 1
Locations of measurement sites in Qingdao (left map, Shandong; right map, Qingdao; 1, Huangdao; 2, Chengyang; 3, Licang; 4, Sifang; 5, Laoshan; 6, Shinan East; 7,Shibei; 8, Shinan West; 9, Yangkou).

TABLE 1
Characteristics of the monitoring sites.

Monitoring sites	Type of station	Local characteristics
Yangkou	Urban background	Few vehicles; many trees, near the sea
Licang	Industrial site	Steelworks; many vehicles, buildings
Shibei	Urban background	Few vehicles, near the park
Shinan east	Business district	Commercial network intensive area
Sifang	Urban background	Few vehicles; near the park
Shinan west	Urban background	Many buildings, near the school, near the sea
Laoshan	Suburban background	Few vehicles; many trees, near the sea
Huangdao	Suburban residential site	Densely populated; many vehicles;
Chengyang	Traffic	Many vehicles, Industry

Coefficients of Divergence. Recent studies shows that the intra urban spatial distributions of atmospheric pollutant concentrations in some study areas are heterogeneous. Coefficients of variation (CV) or a coefficient of divergence (CD) were used to describe the relative heterogeneity of the inter-urban concentration of particles [13]. The CD_{jk} method for identifying the differences of atmospheric pollutant profiles has been described in detail elsewhere [13] (Wilson et al., 2005) and is defined as follows:

$$CD_{jk} = \sqrt{\frac{1}{p}\sum_{i=1}^{p}\left(\frac{X_{ij}-X_{ik}}{X_{ij}+X_{ik}}\right)^2} \qquad (1)$$

where xij represents the average concentration of i at site j, j and k represent two sampling sites, and p is the number of observations [14]. If the value of CD_{jk} approaches zero, the atmospheric pollutant composition in j and k are similar, and if it approaches one, they are significantly different [7]. Therefore, the CD_{jk} could provide a relative measure of homogeneity in the concentration fields. In addition, a threshold of CD_{jk} = 0.2 is used to distinguish homogeneity and heterogeneity between sites (REF) [13] (Wilson et al., 2005).

Spatial Autocorrelation. Observations at different locations may not be independent. For example, measurements made at nearby locations may be closer in value than measurements made at locations farther apart. This phenomenon is called spatial autocorrelation, which can be measured by Moran's I [15,16].

Spatial autocorrelation measures the correlation of a variable with itself through space. Spatial autocorrelation can be positive or negative. Positive spatial autocorrelation occurs when similar values occur near one another while negative spatial autocorrelation indicates dissimilar values. The spatial autocorrelation method for identifying the correlation of atmospheric pollutant profiles was described in detail elsewhere [17]. It covers global spatial autocorrelation (Global Moran's I (GMI)), which is defined as follows.

The global Moran's I statistic is based on cross-products of the deviations from the mean and is calculated for n observations on a variable x at locations j, k as:

$$I = \frac{n}{S_0}\frac{\sum_j\sum_k w_{jk}(x_j-\bar{x})(x_k-\bar{x})}{\sum_j (x_j-\bar{x})^2} \qquad (2)$$

where $\bar{x}$ is the mean of the all x variable, w_{jk} are the elements of the weight matrix, and S_0 is the sum of the elements of the weight matrix:

$$S_0 = \sum_j\sum_k w_{jk} \qquad (3)$$

In general, Moran's I is similar but not equivalent to a correlation coefficient. Its value varies between -1 and 1, representing negative and positive spatial autocorrelation, respectively. Positive and significant Moran's I values mean that nearby areas have similar spatial patterns, whereas negative values indicate the contrary. If the Moran's I is zero, it means the values are arranged randomly.

Since the Moran' I statistic follows a random distribution or a near-normal distribution, the significance test can be converted into the Z value of the normal distribution statistic. If the Z value at the 5% significance level is greater than 1.96 or less than -1.96, they indicate that there is a spatially significant positive or negative correlation between the observations. Values between -1.96 and 1.96 indicate a non-significant spatial correlation of the study. It is extremely significant when values are greater than 2.58. The standard statistic Z is calculated by the following formula:

$$Z = \frac{I-E(I)}{\sqrt{VAR\ (I)}} \qquad (4)$$

Where E (I) and VAR (I) are expectation and variance of Moran'I, respectively, and E (I) = (-1)/(n-1). When Z is positive and significant, it indicates that there is a positive spatial correlation, and the observed values are aggregated. On the contrary, Z is negative and significant, indicating that there is a negative correlation, and the observations tend to be discretely distributed. Z = 0 means that the observations are randomly distributed.

Due to the continuous spatial distribution of $PM_{2.5}$, the concentration is very important for health impact assessment of $PM_{2.5}$ exposure and other purposes [18]. It has been reported by Global Burden of Disease that fine particulate matter ($PM_{2.5}$) is the seventh largest important death risk factor in the world and the fourth largest important death risk factor in China [19,20]. Therefore, to better reflect the spatio-temporal changes of $PM_{2.5}$ concentrations, the Global Moran's I was employed to identify spatial autocorrelation of $PM_{2.5}$ concentrations in Qingdao. Meanwhile, the analysis of spatial autocorrelation could help to analyze whether sparse ground monitoring sites can meet the requirements.

Spatial distribution estimation of $PM_{2.5}$ concentration. Conventional regression analysis can only provide "average" and "global" parameter estimates, rather than "local" parameter estimates, which vary over space in some spatial systems. Geographically weighted regression (GWR) is a relatively simple but effective new technique for exploring spatial nonstationarity. It allows different relationships to exist at different points in space. Therefore, local rather than global parameters can be estimated and spatial uncertainties examined. To solve the problem that the geographic weighting regression (GWR) model cannot overcome the influence of outliers in the small sample data, spatial distributions of the average atmospheric pollutant concentrations for 2015 were simulated using ordinary kriging.

Data analysis was performed using the Data Processing System 9.5 (DPS). For the spatial autocorrelation and agglomeration analysis, the GeoDA1.4.0 and Arc GIS 10.2 were used. The results were displayed using ArcView 4.0. The relationships between the atmospheric pollutants concentration were explored by Spearman rank correlation coefficient.

RESULTS AND DISCUSSION

Temporal variation. Seasonal variation. Ordinary season divisions in China are as follows: spring refers to March to May, summer covers June to August, autumn refers to September to November, and winter covers December to February. As the four seasons in Qingdao are clearly classified, one year is divided according to ordinary season divisions to analyze seasonal variation across Qingdao and in diverse regions. Table 2 shows the descriptive statistics of seasonal average atmospheric pollutant concentration averaged over the 9 sites in Qingdao.

The average $PM_{2.5}$ and PM_{10} concentrations were 51.27 μg/m^3 and 97.55 μg/m^3, aggregated from 9 monitoring sites for the entire year 2015. These values exceed the Chinese National Ambient Air Quality Standards (AAQS) Level-2 (35 μg/m^3 for $PM_{2.5}$ and 70 μg/m^3 for PM_{10}). In addition, NO_2 and SO_2 were also analyzed; their concentrations are 33.34 μg/m^3 and 27.52 μg/m^3 and are thus below the AAQS Level-2 (40 μg/m^3 for NO_2 and 60μg/m^3 for SO_2).

$PM_{2.5}$ and PM_{10} values in Qingdao showed distinct seasonal variations. In general, the atmospheric pollutant concentrations showed a pattern of "high in spring and winter, while low in summer and autumn". Seasonal mean values of $PM_{2.5}$ and PM_{10} concentrations varied from 33.70 μg/m^3 and 72.52 μg/m^3 in summer to 81.37 μg/m^3 and 132.91 μg/m^3 in winter with the latter two being 2.41 and 1.83 times of the former two values. For NO_2 and SO_2, the seasonal average concentrations varied from 22.78 μg/m^3 and 20.64 μg/m^3 in summer to 44.61 μg/m^3 and 44.64 μg/m^3 in winter with the latter two being 1.96 and 2.16 times of the former two values.

In winter and spring, the atmospheric stratification is relatively stable, and the horizontal diffusion is weakened, so the atmospheric pollutant concentration is high. In summer, due to the influence of the subtropical high in the western Pacific, the atmospheric is diffused and the air pollutants are diluted. In addition, Qingdao is a coastal city located on the south Shandong peninsula facing the Yellow Sea on the southeast. Therefore, under the influence of the ocean current and the southeast monsoon climate, most parts of the city are exposed to an ocean

TABLE 2
Descriptive statistics of seasonal average atmospheric pollutants concentrations (unite, μg/m^3).

		$PM_{2.5}$	PM_{10}	NO_2	SO_2
Full year	Min	43.28	81.18	16.68	18.82
	Max	59.97	118.24	42.22	37.41
	Median	45.81	93.98	31.62	23.47
	Mean	51.27	97.55	33.34	27.52
	S.D.	5.54	13.20	7.81	6.31
Spring	Min	28.95	69.38	12.99	11.20
	Max	63.07	147.03	53.34	43.35
	Median	45.81	99.11	37.30	22.79
	Mean	46.32	101.77	33.39	23.02
	S.D.	5.44	12.24	12.07	7.16
Summer	Min	22.71	48.45	6.27	10.80
	Max	41.06	94.42	43.05	44.03
	Median	34.03	72.23	24.86	20.50
	Mean	33.70	72.52	22.78	20.64
	S.D.	3.91	11.68	8.31	6.04
Autumn	Min	20.17	46.84	3.81	10.57
	Max	69.14	119.12	50.57	38.28
	Median	45.49	80.47	29.30	21.18
	Mean	43.14	83.00	32.21	21.45
	S.D.	5.71	16.34	9.78	4.77
Winter	Min	60.19	99.16	15.51	26.96
	Max	126.73	192.67	65.19	71.35
	Median	76.38	130.00	46.78	41.05
	Mean	81.37	132.91	44.61	44.64
	S.D.	9.91	17.65	9.65	11.42

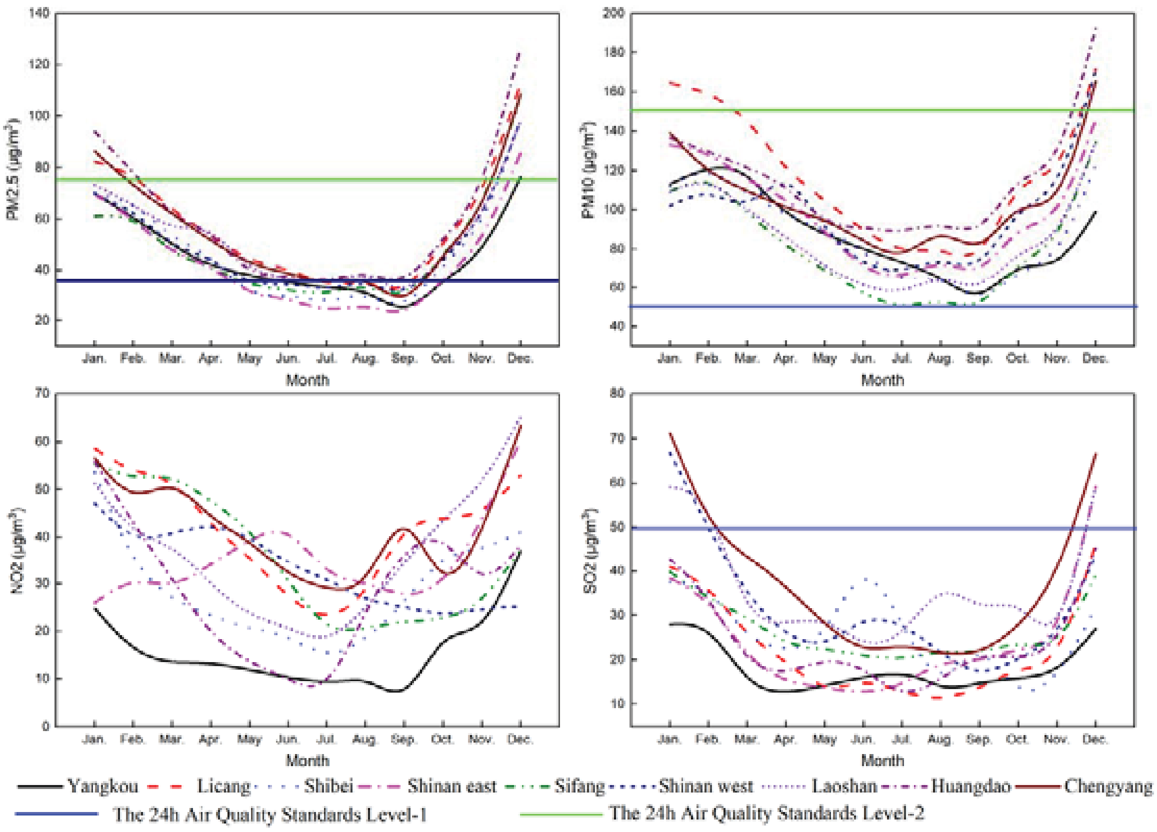

FIGURE 2
Monthly variations of atmospheric pollutants in 9 different regions of Qingdao.

climate with high humidity and abundant precipitation in summer [21]. So the atmospheric pollutants deposit and diffuse more easily in summer due to abundant rainfall and the strong air convection. In winter, however, the low temperature and insufficient photochemical promotion contribute a dominant downdraft, resulting in insufficient air diffusion and stronger emissions of primary particles [22]. At the same time, the coal combustion affects Qingdao in winter, leading to a seasonal high of the PM in Qingdao.

Monthly variation. The monitored monthly variations of four atmospheric pollutant concentrations at urban sites are presented in Figure 2. As can be seen, the four atmospheric pollutant concentrations showed a U-shaped pattern of "high in autumn and winter but low in spring and summer", especially $PM_{2.5}$, PM_{10} and SO_2. Furthermore, according to AAQS (GB 3095-2012), only a few sites exceeded the 24h Air Quality Standards Level-2 for atmospheric pollutants (75 μg/m³ for $PM_{2.5}$, 150 μg/m³ for PM_{10}, 80 μg/m³ for NO_2 and 50 μg/m³ for SO_2) in a few months. It's worth noting that NO_2 concentrations were below the 24h Air Quality Standards Level-1 (80 μg/m³).

As shown, the monthly averages were similar among the different regions. There were two important time inflections that should be followed in January and September. There was a downward trend after January, which was basically stable, but a slightly decreasing trend from June to September and an apparently increasing trend after September. For $PM_{2.5}$, the lowest monthly average concentration was observed in September in Shinan east (20.17 μg/m³), reaching the air quality of the 24h Air Quality Standards Level-2 and the highest value was found in December in Huangdao (126.73 μg/m³). For PM_{10}, the lowest monthly average concentration was observed in September in Sifang (46.84 μg/m³), reaching the air quality of the 24h Air Quality Standards Level-1 and the highest value was found in December in Huangdao (126.73 μg/m³). For NO_2, the lowest monthly average concentration was observed in September in Yangkou (3.81 μg/m³), reaching the air quality of the 24h Air Quality Standards Level-1 and the highest value was found in December in Laoshan (65.19μg/m³). For SO_2, the lowest monthly average concentration was observed in September in Shibei (10.57μg/m³), reaching the air quality of the 24h Air Quality Standards Level-1 and the highest value was found in January in Chengyang (71.35μg/m³).

Combined with Qingdao's monthly average $PM_{2.5}/PM_{10}$ in 2015, the ratio of each monitoring point reached a peak on the time scale from December to January, indicating that the "Heating" contributed significantly to $PM_{2.5}$, during the winter heating process. In addition to generating atmospheric particulate matter, a large amount of gaseous pollutants such as SO_2 are emitted simultaneously, which contributes to the formation of secondary $PM_{2.5}$. For the NO_2/ SO_2 ratio, the peaks and valleys of the monitoring points on the time scale are not exactly the same. For the entire city, the higher ratios are October, November and May. This period is during the tourist season, and the traffic volume has increased significantly, resulting in a large amount of nitrogen dioxide emissions; the lowest proportion is from January to February, which is the winter heating period. When coal is burnt a large amount of sulfur dioxide is produced, which reduces its proportion.

Brunekreef and Holgate (2002) [22] pointed out that meteorological effects could affect monthly variation, because climate changes can affect the accumulation, diffusion, sedimentation, and chemical conversion of pollutants in the atmosphere. Studies have shown that the differences in physical properties between surface water and land will cause local atmospheric movements, forming weather phenomena with significant daily changes such as sea and land breeze, lake and land breeze, and river breeze [24-27]. The existence of such local atmospheric movements will cause changes in wind direction, wind speed in the area, and affect the distribution of air pollutant concentrations in the area. The urban area of Qingdao is in the typical East Asian monsoon climate zone. The weather and climate are influenced by the sea and land and have the transitional characteristics between continental and oceanic. In general, the concentration of pollutants at coastal monitoring sites is lower than that at inland monitoring sites.

Daily variations. The monitored daily variations of four atmospheric pollutant concentrations at urban sites are presented in Figure 3. In order to compare changes in short-term variation in different regions, this section has also used the Min-Max Normalization method to standardize 0-1 concentrations of four atmospheric pollutants in each region (Figure 3 a, b, c and d). As shown in the figures, the daily average of the four atmospheric pollutant concentrations showed cyclical and pulse-like changes in different urban sites of Qingdao in 2015. For $PM_{2.5}$, the daily minimum value was detected on August 09th at 4.77 μg/m^3 in Shibei, while the maximum was detected on December 24th at 376.46 μg/m^3 in Huangdao. For PM_{10}, the daily minimum value was observed on July 22th at 16.17 μg/m^3 in Shinan west,

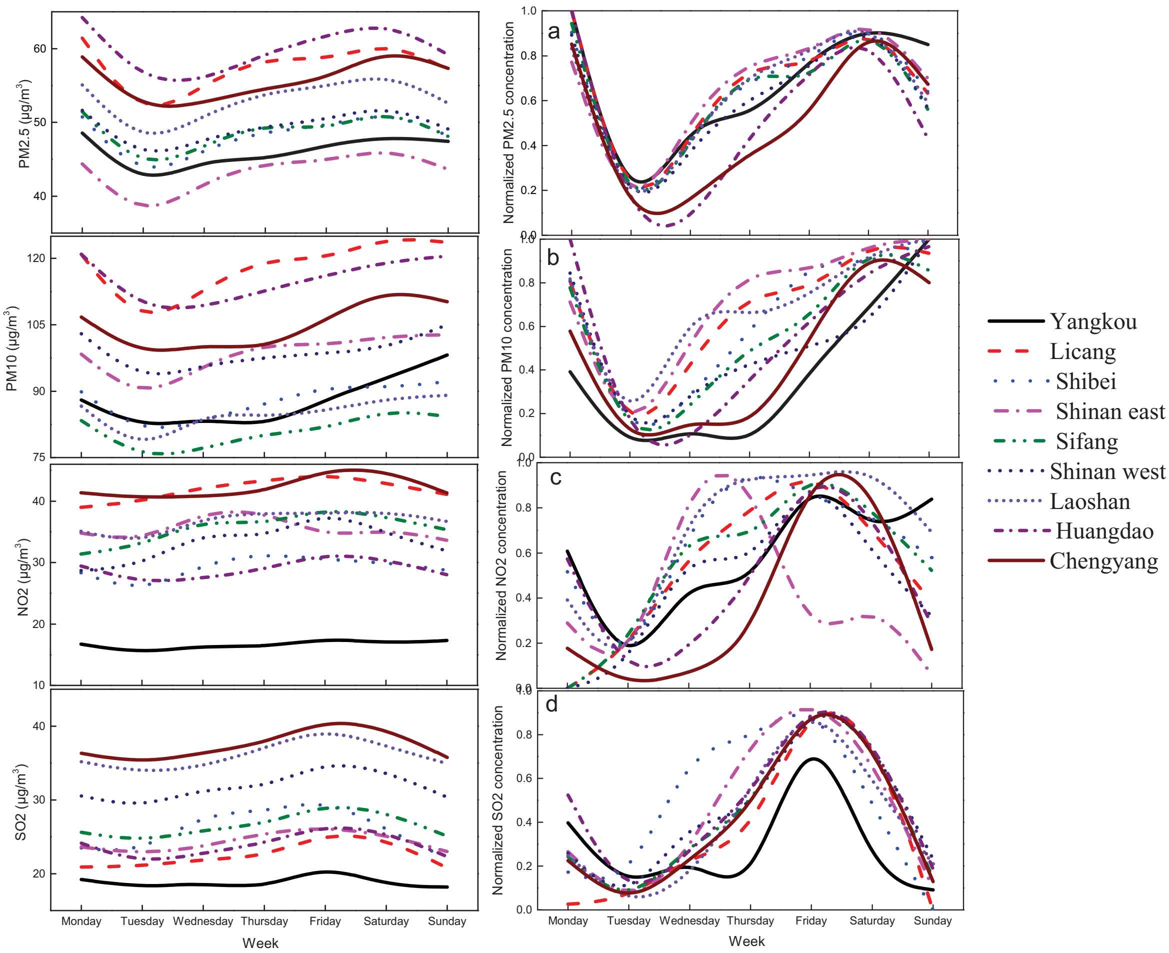

FIGURE 3
Daily variations of atmospheric pollutants in 9 different regions of Qingdao (a, b, c, d are standardized concentration for $PM_{2.5}$, PM_{10}, NO_2 and SO_2 in each region).

while the maximum value was also observed on December 24th at 478.58 μg/m^3 in Huangdao. For NO_2, the daily minimum value was found on June 22th at 1.65 μg/m^3 in Huangdao and the maximum was found on February 11th at 242.11 μg/m^3 Sifang. For SO_2, the daily minimum value was detected on June 23th at 1.38 μg/m^3 in Huangdao, while the maximum value was detected on January 09th at 184.03 μg/m^3 in Laoshan. However, based on the average of the four pollutant concentrations in 2015, there were more days of excellent quality in summer in Qingdao, followed by autumn, and spring, while the fewest days of good quality took place in winter. Combined with Qingdao urban average Air Quality Index (AQI), summer witnessed better air quality reaching a standard of 87, followed by autumn (77 days), spring (71 days). Winter was the worst season in terms of air quality reaching the standard of 51 days. The region with a slight pollution was Huangdao, obviously, where 20 heavily and 22 moderately polluted days were observed in 2015.

Diurnal variations. In order to compare the diurnal variations of different regions, the values of the four atmospheric pollutant concentrations were summarized by every hour and were 0-1 standardized using the Min-Max Normalization method for each region and the results are presented in Figure 4. Compared with monthly variations of four atmospheric pollutant concentrations, diurnal variations of $PM_{2.5}$ and NO_2 shared great resemblance with bimodal pattern in different regions though the degree of change varies greatly. Generally, the extent of the variation was greater during daytime than during the night. Moreover, there was an apparently increasing trend after 5:00 am, occurring during the early morning rush hour. The peak in the morning appears around 9:00 am, which is due to enhanced anthropogenic activity during the rush hour. Then they have been falling, which may be due to the higher sea breeze frequency after 13:00 pm, which is conducive to reducing the concentration of atmospheric pollutants. For $PM_{2.5}$ and NO_2, most monitoring sites showed second highest peaks around 19:00 to 21:00 pm, similar to those observed in Beijing and New York City [28,29]. For PM_{10} and SO_2, most monitoring sites showed concentrations in an unimodal pattern with a significant peak between 5:00 and 10:00 pm.

Weekend effect. Intense human activities can affect weather and climate in many ways. The more typical is the weekend effect, defined as the average concentration for Saturday through Monday minus the average concentration for Wednesday through Friday [30,31] . Szulejko et al. (2018) [32] analyzed the hourly data of NO, NO_2, O_3 and CO using the data acquired in the Yong-San district of Seoul, Korea from 2009 to 2013 and found the weekend effect.

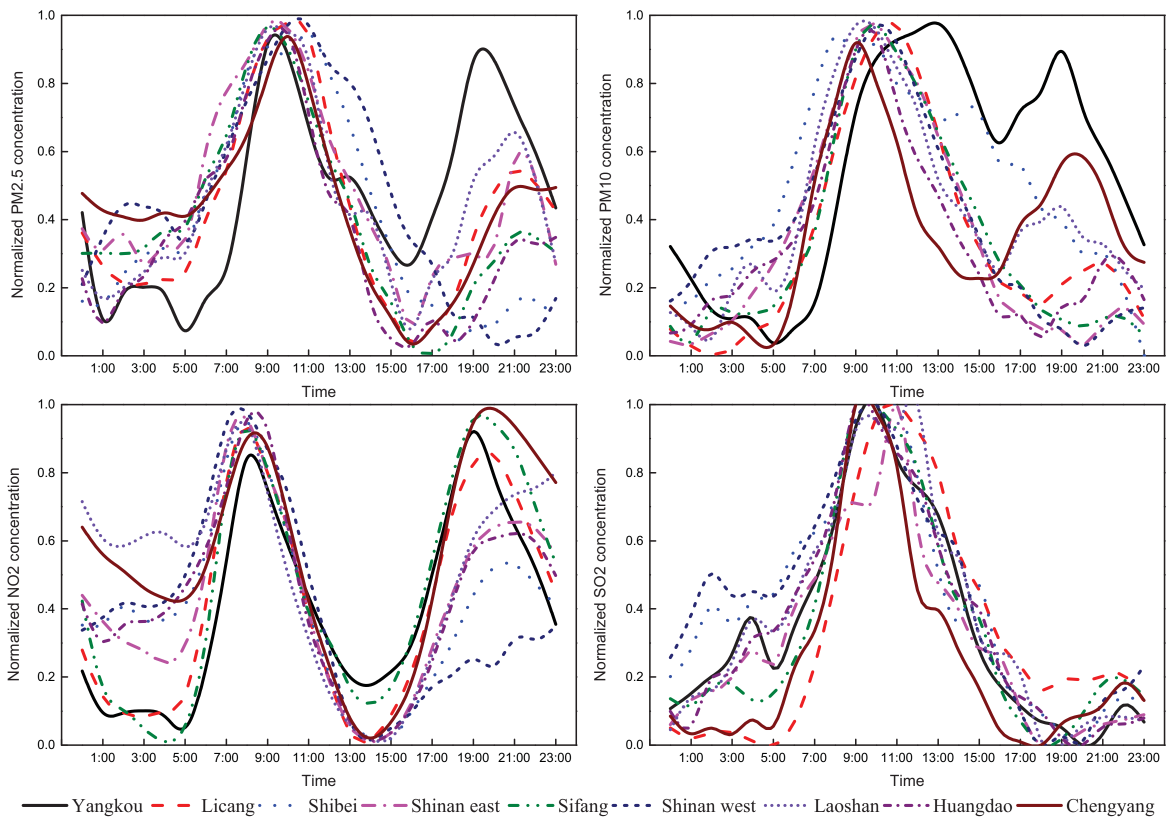

FIGURE 4
Diurnal variations of atmospheric pollutants in 9 different regions of Qingdao (Beijing time).

TABLE 3
Weekday and weekend differences in $PM_{2.5}$, PM_{10}, NO_2 and SO_2 concentrations at nine stations.

Stations	Weekday (μg/m³)				Weekend(μg/m³)				Weekend (%)			
	$PM_{2.5}$	PM_{10}	NO_2	SO_2	$PM_{2.5}$	PM_{10}	NO_2	SO_2	$PM_{2.5}$	PM_{10}	NO_2	SO_2
Yangkou	45.64	84.63	16.81	19.31	48.03	93.02	16.97	18.56	5.25	9.91	0.92	-3.86
Licang	57.48	117.58	43.33	23.25	59.90	123.18	40.98	22.14	4.22	4.76	-5.43	-4.76
Shibei	48.27	87.21	30.61	28.95	50.21	90.93	29.04	23.84	4.03	4.27	-5.13	-17.67
Shinan East	43.77	99.04	36.95	25.17	44.90	101.17	34.66	23.96	2.57	2.15	-6.22	-4.80
Sifang	48.57	79.60	37.35	27.36	50.51	84.53	34.72	26.35	3.99	6.20	-7.04	-3.66
Shinan West	49.22	97.37	35.87	32.83	51.07	102.54	31.78	31.60	3.76	5.32	-11.40	-3.75
Laoshan	53.32	85.02	37.82	37.11	54.85	88.00	36.70	35.78	2.86	3.50	-2.98	-3.59
Huangdao	58.93	112.57	29.29	24.52	62.38	120.23	29.33	24.03	5.85	6.80	0.13	-1.95
Chengyang	54.37	102.03	42.47	38.34	58.82	110.08	42.59	37.26	8.18	7.89	0.28	-2.80

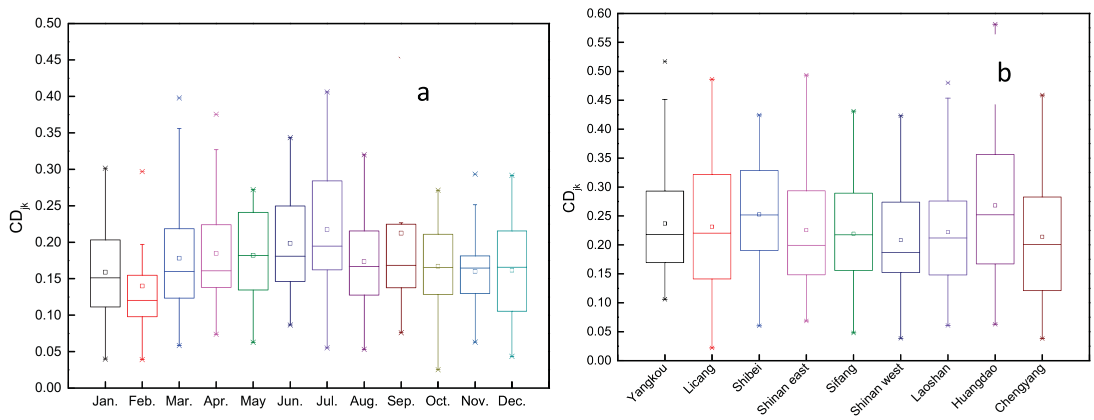

FIGURE 5
Coefficients of divergence for atmospheric pollutants (a, calculated across all urban sites pairs by month for the entire study (Jan.—Dec. 2015); b, calculated across all months pairs by different urban sites). Whisker-box plot as described previously.

From the weekly variation of $PM_{2.5}$ and PM_{10} (Figure 3 a, b), it can be seen that the $PM_{2.5}$ and PM_{10} concentrations at each site began to accumulate on Wednesday, reached their maximum on the weekend and rapidly decreased on Monday. However, for NO_2 and SO_2, the concentrations reached their maximum on weekdays and declined on weekends. The main reason is that these urban sites are located in urban areas where human activities are concentrated. The traffic flow on working days is large and frequent. On weekends, the traffic flow is reduced drastically and the emissions of automobile exhausts are declining. Combined with the definition of the above mentioned weekend effect, WE= $(C_{weekend}-C_{weekday})/C_{weekday}$, this paper has calculated the weekend effect of atmospheric pollutants from 9 stations in Qingdao (Table 3). As shown in Table 3, the trends for $PM_{2.5}$, PM_{10}, and SO_2, at these sites are consistent with visible weekend effects. Clearly, the concentration of SO_2 on weekends is higher than on working days, and the concentration of NO_2 on weekends is significantly reduced. It is speculated that the change of motor vehicle emissions on weekends and working days may be the main reason for the $PM_{2.5}$ weekend effect.

Spatial variation. Coefficients of Divergence (CD) calculations for atmospheric pollutants. The coefficient of divergence can be used to measure the spread of the data points for two datasets. The monthly CD_{jk}s were calculated across all urban site pairs for the whole daily data of the study (Figure 5). The median CD_{jk} values ranged from 0.120 to 0.195

suggesting a homogeneous-to modestly heterogeneous distribution of atmospheric pollutants for the 9 sites. With the exception of February, May and July, the range between the 1st and 3rd quartiles was approximately 0.16. The median CD_{jk} values during the summer and winter seasons were 0.179 and 0.145, respectively. Furthermore, the average median CD_{jk} value of all urban sites was 0.165 during the whole year, proposing spatial homogeneity (Figure 5a). This suggests that exposures to the four atmospheric pollutants in the urban core sites may be well-estimated using a central monitoring site at least for 24-h-based concentrations. Moreover, as seen from Figure 5, the CD_{jk} values did not seem to change significantly in each season (average CD_{jk} values were 0.196 and 0.154 for summer and winter, respectively).

In order to compare the monthly variations within one site, the reginal CD_{jk}s were calculated across all months' pairs (Figure 5b). As shown in the Figure 5, the conversion range is quite large between different months, especially Licang (CDmin = 0.022, CDmax = 0.486) and Hunagdao (CDmin = 0.062, CDmax = 0.581). And the median CD_{jk} values greater than approximately 0.2 were indicative of a relatively heterogeneous temporal distribution, which can further explain Figure 2.

Spatial autocorrelation analysis. Moran's I scatter plots of the $PM_{2.5}$ concentrations in Qingdao using GeoDA are presented in Table 4. Results showed, that for $PM_{2.5}$ Moran's I was greater than 0 for hourly, annual, seasonal, and monthly values in 2015, except for April, August, September, October, and December, which were close to 0 indicating no significant spatial autocorrelation. The remaining months ranged from 0.114 to 0.423 and the hours ranged from 0.115 to 0.315, suggesting a significant but less strong positive spatial autocorrelation of $PM_{2.5}$ concentrations in Qingdao. The hourly and monthly average Z(I) values were 1.61 and 1.53, which did not exceed 1.96, indicating a non-significant spatial correlation. Therefore, the pollution of Qingdao could be comprehensively reflected showing no significant spatial heterogeneity among the sites. This further verified the analysis of section 3.2.1. In addition, these results indicated that the $PM_{2.5}$ pollution source was not generated by individual sites, but there were many sources of pollution widely distributed throughout the urban area, or sources of pollution from outside the city. It can be concluded that air pollutants in urban areas are not produced at specific local sites.

TABLE 4
Spatial autocorrelation index of $PM_{2.5}$ concentrations in Qingdao in 2015.

Hourly	0h	1h	2h	3h	4h	5h	6h	7h	8h	9h	10h	11h
Moran's I-$PM_{2.5}$	0.257	0.163	0.201	0.169	0.162	0.116	0.115	0.118	0.141	0.219	0.244	0.173
P	0.043	0.099	0.063	0.087	0.088	0.125	0.133	0.137	0.116	0.066	0.055	0.089
Z	1.896	1.407	1.644	1.487	1.462	1.231	1.215	1.203	1.330	1.716	1.828	1.482
Hourly	12h	13h	14h	15h	16h	17h	18h	19h	20h	21h	22h	23h
Moran's I-$PM_{2.5}$	0.179	0.213	0.126	0.139	0.130	0.138	0.225	0.281	0.315	0.264	0.249	0.268
P	0.081	0.048	0.118	0.102	0.099	0.088	0.050	0.035	0.033	0.049	0.053	0.039
Z	1.531	1.799	1.297	1.402	1.410	1.437	1.865	2.114	2.226	1.919	1.848	1.959
Monthly	Jan.	Feb.	Mar.	Apr.	May	Jun.	Jul.	Aug.	Sep.	Oct.	Nov.	Dec.
Moran's I-$PM_{2.5}$	0.264	0.171	0.2	-0.09	0.373	0.423	0.319	0.058	0.065	0.099	0.114	0.081
p	0.027	0.091	0.079	0.436	0.018	0.004	0.013	0.198	0.175	0.147	0.129	0.156
Z	2.143	1.521	1.648	0.084	2.482	2.761	2.445	0.893	0.924	1.127	1.214	1.109
Seasonal	Spring	Summer	Autum	Winter	Annual							
Moran's I-$PM_{2.5}$	0.303	0.289	0.119	0.177	0.250							
P	0.044	0.032	0.130	0.080	0.037							
Z	2.120	2.085	1.227	1.614	1.896							

Spatial distribution of atmospheric pollutants concentrations in urban of Qingdao. Because monitoring sites are clustering in the urban areas of Qingdao, the four pollutant concentrations are able to reflect the distribution of pollutants in the urban areas of Qingdao. Spatial distribution of average atmospheric pollutant concentrations in 2015 were simulated using Ordinary Kriging. The research of Liao et al. (2006) [33] showed that their investigation of GIS approaches for estimating daily mean geocoded location-specific air pollutant concentrations supports the use of a spherical model to perform lognormal ordinary kriging on a national scale. Zongwei Ma et al., (2014) [34] successfully applied this approach for simulating the spatial distribution of $PM_{2.5}$ using satellite remote sensing in China. And Lü and Tian (2007) [35] found that during the period 1990 to 2003, ambient air NO_2 concentrations were significantly enhanced in urban observatories as a result of anthropogenic influences.

In this study, $PM_{2.5}$ was used as an example to simulate the concentration change in urban areas. The results of Ordinary Kriging are shown in urban areas covered by monitoring sites (Figure 6). As shown in the Figure 6, the concentrations of pollutants in inland areas are high, while they are lower near the seashore. Furthermore, it is obvious that most parts of urban Qingdao suffer from severe air pollutions in winter, especially the buffer of Huangdao, Chengyang and Licang.

Correlation between PM and gaseous pollutant. It has been found that the correlations between PM and gaseous pollutants could indicate the source types of particulates: positive correlations indicate the same sources, whereas negative correlations imply different sources, or the gaseous pollutant(s) may be the precursors or oxides in the process of particulate nucleation and growth [36,37]. Partial correlation coefficients between particulates and gaseous pollutants are shown in Table 5. All coefficients shown have gone through the test of significance. SO_2 mainly derived from stationary pollution sources that originate mainly from heating emission sources and other industrial emission sources [38-40]. Unlike SO_2, NOx has its main source in mobile pollution referring to on-road mobile sources, especially heavy duty diesel vehicle emissions [41,42]. CO could be seen as kind of mixed pollution source. Because it emits directly from incomplete combustion such as biomass and fossil fuel burning, or indirectly from the oxidation of methane and volatile organic compounds (VOCs) [43]. And O_3 is known as a product from the photochemistry reaction of NOx, CO and VOCs [44,45].

As shown in Table 5, the correlations between PM and SO_2, NO_2 were positive, indicating that throughout the year, PM originated mainly from direct sources such as stationary and/or mobile emissions. $PM_{2.5}$ and PM_{10} were strong positively correlated with CO ($p<0.01$) in all months, suggesting strong contributions of mixed combustion sources to fine and coarse particulates. $PM_{2.5}$ was negatively correlated with O_3 in several months and throughout the year. Because O_3 plays an important role in the growth of ultrafine particulates, like photochemistry

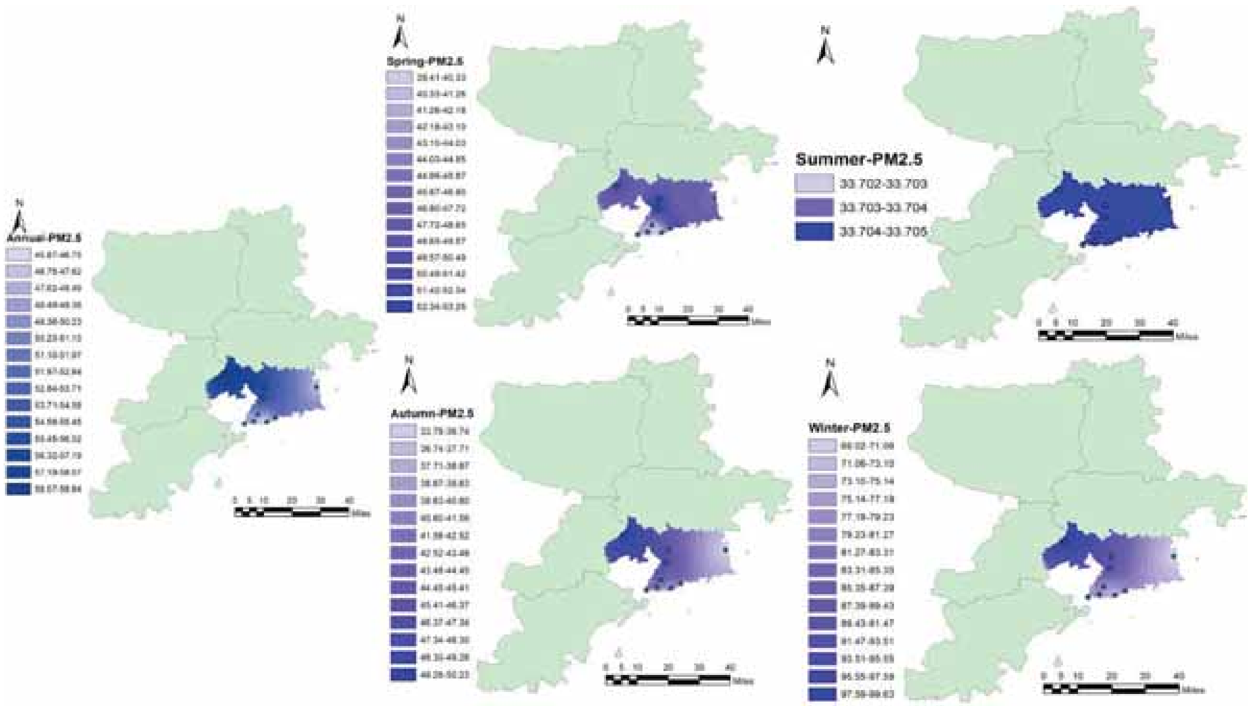

FIGURE 6
Spatial distribution of average $PM_{2.5}$ concentration in annual, spring, summer and winter (2015) (unit: μg/m^3)

TABLE 5
Correlations between PM and gaseous pollutants.

TIME	Index	SO2	NO2	CO	O_3-8h	Index	SO_2	NO_2	CO	O_3-8h
Jan.		0.580**	0.599**	0.949**	-0.484**		0.577**	0.601**	0.902**	-0.505**
Feb		0.475**	0.552**	0.778**	-0.116		0.404**	0.363**	0.570**	-0.068
Mar		0.531**	0.499**	0.853**	0.225		0.452**	0.443**	0.843**	-0.005
Apr		0.484**	0.375**	0.755**	0.478**		0.352**	0.322**	0.256	0.529**
May		0.415**	0.372**	0.799**	0.619**		0.357**	0.418**	0.828**	0.704**
Jun		0.339**	0.346**	0.762**	0.716**		0.286**	0.385**	0.833**	0.784**
Jul	$PM_{2.5}$	0.229**	0.228**	0.765**	0.849**	PM_{10}	0.113**	0.200**	0.794**	0.891**
Aug		0.257**	0.190**	0.822**	0.764**		0.187**	0.292**	0.874**	0.814**
Sep		0.431**	0.421**	0.848**	0.594**		0.334**	0.436**	0.831**	0.608**
Oct		0.267**	0.257**	0.875**	0.468**		0.330**	0.382**	0.833**	0.31
Nov		0.411**	0.502**	0.797**	-0.172		0.492**	0.549**	0.791**	-0.069
Dec		0.511**	0.590**	0.965**	-0.361*		0.569**	0.562**	0.979**	-0.427*
Annual		0.471**	0.474**	0.924**	-0.211**		0.425**	0.471**	0.801**	0.016

Significant correlation at the *P <0.05 and **P < 0.01 levels.

process [46]. Therefore it promotes the transformation of fine particles to large particles. PM_{10} was positively correlated with O_3 in most months, indicating opposite sources of fine particulates, such as direct exhaust rather than homogeneous or heterogeneous reactions.

CONCLUSION

In general, the four atmospheric pollutant concentrations in Qingdao had an apparent U-shaped pattern of "high in autumn and winter but low in spring and summer", and the double-peak or single-peak impulse-shaped daily variation. Their annual average concentrations in 2015 across Qingdao were 51.27 μg/m^3 ($PM_{2.5}$), 97.55 μg/m^3 (PM_{10}), 33.34 μg/m^3 (NO_2) and 27.52 μg/m^3 (SO_2), reaching the national Grade II standard, respectively.

The four atmospheric pollutant concentrations changed significantly in both long-term and short-term scales. Their pollution level varied greatly in different seasons. In winter, their concentrations were the highest, followed by those of autumn and spring, both reaching the national Grade II standard, whereas their concentrations in summer were the lowest, at the national Grade I standard, except PM_{10}. Monthly variations were similar at different monitoring sites, showing U-shaped patterns. The monthly average $PM_{2.5}$ concentration reached a minimum in September and a maximum in December, the same was true for PM_{10}. For NO_2 and SO_2, the lowest monthly average concentrations were observed in July and August, reaching the air quality of the 24h Air Quality Standards Level-1. The highest values were found in January.

However, daily variation shared the same bimodal or unimodal pattern regardless of seasonal change. Throughout the day, the four atmospheric pollutant concentrations were highest around 08:00-10:00 am and lowest around 14:00-18:00 pm. For $PM_{2.5}$ and PM_{10}, the daily peak during the year happened on December 24th in Huangdao (376.46 μg/m^3, 478.58 μg/m^3), while the minimum value appeared on August 09th in Shibei (4.77 μg/m^3 for $PM_{2.5}$) and July 22th in Shinan west (16.17 μg/m^3 for PM_{10}). For NO_2 and SO_2, the daily minimum value was detected on June 22th and 23th in the year in Huangdao (1.65 μg/m^3, 1.38 μg/m^3), while the daily peak was detected on February 11th in Sifang (242.11 μg/m^3 for NO_2) and January 09th in Laoshan (184.03 μg/m^3 for SO_2). Air quality in Qingdao City was worse on weekends than on weekdays. $PM_{2.5}$ and PM_{10} concentrations were lower on weekdays than on weekends while SO_2 concentrations were higher on weekdays than on weekends, indicating a "weekend effect".

The spatial correlation theory was used to study the spatial correlation of air pollutants at nine environmental monitoring points in urban areas of Qingdao. After calculating the Moran index, it was found that the spatial correlation of pollutants at each monitoring point was not strong, showing that air pollutants in urban areas are not produced in the specific local site. The spatial distribution by Ordinary Kriging displayed that most parts of urban Qingdao suffer from severe air pollutions in winter and the concentrations of pollutants in inland areas are higher than in seaside sites, especially the buffer of Huangdao, Chengyang and Licang.

ACKNOWLEDGEMENTS

Author Contributions: Data curation,Y.X.; Funding acquisition, X.Z. and Y.W.; Investigation, X.L.; Methodology, X.L.; Project administration, X.Z.; Software, X.L.; Supervision, X.L.; Visualization, Y.W.; Writing—original draft, X.Z. and Y.W.; Writing—review & editing, X.L.

Funding: The work is funded by National Natural Science Foundation of China (42101470), the Research Project of the Ministry of Science and Technology of China (2019YFC0507800), the Germany Federal Ministry of Transport and Digital Infrastructure (BMVI) as part of SmartAQnet (19F2003B), the Support Project of High-level Teachers in Beijing Municipal Universities in the Period of 13th Five - year Plan (CIT& TCD 201904037).

We would like to acknowledge Beijing Key Laboratory of Big Data Technology for Food Safety for providing a research grant to conduct this work. We express gratitude to the editors for the editing assistance. Lastly, we would like to thank the reviewers for their valuable comments and suggestions on our paper.

REFERENCES

[1] Almeida, S. M., Pio, C. A., Freitas, M. C., Reis, M. A., and Trancoso, M. A. (2005). Source apportionment of fine and coarse particulate matter in a sub-urban area at the Western European Coast. Atmospheric Environment. 39(17), 3127-3138.

[2] Wilson, W. E., and Suh, H. H. (1997). Fine particles and coarse particles: concentration relationships relevant to epidemiologic studies. Journal of the Air & Waste Management Association. 47(12), 1238-1249.

[3] Pope III, C. A., Burnett, R. T., Thun, M. J., Calle, E. E., Krewski, D., Ito, K., and Thurston, G. D. (2002). Lung cancer, cardiopulmonary mortality, and long-term exposure to fine particulate air pollution. Jama. 287(9), 1132-1141.

[4] Perez, L., Medina-Ramón, M., Kunzli, N., Alastuey, A., Pey, J., Pérez, N., and Sunyer, J. (2009). Size fractionate particulate matter, vehicle traffic, and case-specific daily mortality in Barcelona, Spain. Environmental Science & Technology. 43(13), 4707-4714.

[5] Zanobetti, A., and Schwartz, J. (2009). The effect of fine and coarse particulate air pollution on mortality: a national analysis. Environmental Health Perspectives. 117(6), 898-903.

[6] WHO (2012) IARC: Diesel Engine Exhaust Carcinogenic, I.A.f.R.o.C. (IARC) (Ed.), Lyon, France.

[7] Pakbin, P., Hudda, N., Cheung, K. L., Moore, K. F., and Sioutas, C. (2010). Spatial and temporal variability of coarse (PM10− 2.5) particulate matter concentrations in the Los Angeles area. Aerosol Science and Technology, 44(7), 514-525.

[8] Wang, S., and Hao, J. (2012). Air quality management in China: Issues, challenges, and options. Journal of Environmental Sciences. 24(1), 2-13.

[9] China National Environmental Monitoring Centre (CNEMC) (2015). National Air quality. http://www.cnemc.cn/en/. (Accessed January.2020).

[10] Kim, C. S., Adachi, M., Okuyama, K., and Seinfeld, J. H. (2002). Effect of NO 2 on particle formation in SO 2/H 2 O/air mixtures by ion-induced and homogeneous nucleation. Aerosol Science & Technology. 36(9), 941-952.

[11] Holmes, N. S. (2007). A review of particle formation events and growth in the atmosphere in the various environments and discussion of mechanistic implications. Atmospheric Environment. 41(10), 2183-2201.

[12] Kong, L. D., Zhao, X., Sun, Z. Y., Yang, Y. W., Fu, H. B., Zhang, S. C., and Chen, J. M. (2014). The effects of nitrate on the heterogeneous uptake of sulfur dioxide on hematite. Atmospheric Chemistry and Physics. 14(17), 9451-9467.

[13] Wilson, J. G., Kingham, S., Pearce, J., and Sturman, A. P. (2005). A review of intraurban variations in particulate air pollution: Implications for epidemiological research. Atmospheric Environment. 39(34), 6444-6462.

[14] Krudysz, M., Moore, K., Geller, M., Sioutas, C., and Froines, J. (2009). Intra-community spatial variability of particulate matter size distributions in Southern California/Los Angeles. Atmospheric Chemistry and Physics. 9(3), 1061-1075.

[15] Moran, P. A. (1948). The interpretation of statistical maps. Journal of the Royal Statistical Society. Series B (Methodological). 10(2), 243-251.

[16] Geary, R. C. (1954). The contiguity ratio and statistical mapping. The Incorporated Statistician. 5(3), 115-146.

[17] Xu, G., Jiao, L., Zhao, S., and Cheng, J. (2016). Spatial and temporal variability of PM 2.5 concentration in China. Wuhan University Journal of Natural Sciences. 21(4), 358-368.

[18] Du, Y., and Li, T. (2016). Assessment of health-based economic costs linked to fine particulate (PM 2.5) pollution: a case study of haze during January 2013 in Beijing, China. Air Quality, Atmosphere & Health. 9(4), 439-445.

[19] Cohen, A. J., Ross Anderson, H., Ostro, B., Pandey, K. D., Krzyzanowski, M., Künzli, N., ... and Smith, K. (2005). The global burden of disease due to outdoor air pollution. Journal of Toxicology and Environmental Health, Part A. 68(13-14), 1301-1307.

[20] Lim, S. S., Vos, T., Flaxman, A. D., Danaei, G., Shibuya, K., Adair-Rohani, H., and Aryee, M. (2012). A comparative risk assessment of burden of disease and injury attributable to 67 risk factors and risk factor clusters in 21 regions, 1990–2010: a systematic analysis for the Global Burden of Disease Study 2010. The Lancet. 380(9859), 2224-2260.

[21] Zhang, R., Wang, M., Sheng, L., Kanai, Y., and Ohta, A. (2004). Seasonal characterization of dust days, mass concentration and dry deposition of atmospheric aerosols over Qingdao, China. China Particuology. 2(5), 196-199.

[22] Chai, F., Gao, J., Chen, Z., Wang, S., Zhang, Y., Zhang, J., and Ren, C. (2014). Spatial and temporal variation of particulate matter and gaseous pollutants in 26 cities in China. Journal of Environmental Sciences. 26(1), 75-82.

[23] Brunekreef, B., and Holgate, S. T. (2002). Air pollution and health. The Lancet. 360(9341), 1233-1242.

[24] Avissar, R., and Pielke, R. A. (1989). A parameterization of heterogeneous land surfaces for atmospheric numerical models and its impact on regional meteorology. Monthly Weather Review. 117(10), 2113-2136.

[25] Porson, A., Steyn, D. G., and Schayes, G. (2007). Sea-breeze scaling from numerical model simulations, Part I: Pure sea breezes. Boundary-Layer Meteorology. 122(1), 17-29.

[26] Crosman, E. T., and Horel, J. D. (2010). Sea and lake breezes: A review of numerical studies. Boundary-Layer Meteorology. 137(1), 1-29.

[27] Choi, S. Y., Lee, Y. H., Cho, C., and Kim, K. R. (2015). Analysis of local wind induced by surface heterogeneity and sloping terrain near Nakdong river. Asia-Pacific Journal of Atmospheric Sciences. 51(3), 249-257.

[28] DeGaetano, A. T., and Doherty, O. M. (2004). Temporal, spatial and meteorological variations in hourly PM2. 5 concentration extremes in New York City. Atmospheric Environment. 38(11), 1547-1558.

[29] Zhao, X., Zhang, X., Xu, X., Xu, J., Meng, W., and Pu, W. (2009). Seasonal and diurnal variations of ambient PM2. 5 concentration in urban and rural environments in Beijing. Atmospheric Environment. 43(18), 2893-2900.

[30] Gong, D. Y., Guo, D., and Ho, C. H. (2006). Weekend effect in diurnal temperature range in China: Opposite signals between winter and summer. Journal of Geophysical Research: Atmospheres. 111(D18).

[31] Xia, X., Eck, T. F., Holben, B. N., Phillippe, G., and Chen, H. (2008). Analysis of the weekly cycle of aerosol optical depth using AERONET and MODIS data. Journal of Geophysical Research: Atmospheres. 113(D14).

[32] Szulejko, J. E., Adelodun, A. A., Kim, K. H., Seo, J. W., Vellingiri, K., Jeon, E. C., ... and Brown, R. J. (2018). Short and Long-Term Temporal Changes in Air Quality in a Seoul Urban Area: The Weekday/Sunday Effect. Sustainability. 10(4), 1248.

[33] Liao, D., Peuquet, D. J., Duan, Y., Whitsel, E. A., Dou, J., Smith, R. L., and Heiss, G. (2006). GIS approaches for the estimation of residential-level ambient PM concentrations. Environmental Health Perspectives. 114(9), 1374-1380.

[34] Ma, Z., Hu, X., Huang, L., Bi, J., and Liu, Y. (2014). Estimating ground-level PM2. 5 in China using satellite remote sensing. Environmental Science & Technology. 48(13), 7436-7444.

[35] Lü, C., and Tian, H. (2007). Spatial and temporal patterns of nitrogen deposition in China: synthesis of observational data. Journal of Geophysical Research: Atmospheres. 112(D22).

[36] Zhang, R., Khalizov, A., Wang, L., Hu, M., and Xu, W. (2011). Nucleation and growth of nanoparticles in the atmosphere. Chemical Reviews. 112(3), 1957-2011.

[37] Sun, K., Tao, L., Miller, D. J., Pan, D., Golston, L. M., Zondlo, M. A., and Zhang, Y. (2017). Vehicle emissions as an important urban ammonia source in the United States and China. Environmental Science & Technology. 51(4), 2472-2481.

[38] Huang, Q., Cheng, S., Perozzi, R. E., and Perozzi, E. F. (2012). Use of a MM5–CAMx–PSAT modeling system to study SO 2 source apportionment in the Beijing Metropolitan Region. Environmental Modeling & Assessment. 17(5), 527-538.

[39] Lee, H. D., Yoo, J. W., Kang, M. K., Kang, J. S., Jung, J. H., and Oh, K. J. (2014). Evaluation of concentrations and source contribution of PM10 and SO2 emitted from industrial complexes in Ulsan, Korea: Interfacing of the WRF–CALPUFF modeling tools. Atmospheric Pollution Research. 5(4), 664-676.

[40] Fioletov, V. E., McLinden, C., Krotkov, N., and Li, C. (2015). Lifetimes and emissions of SO2 from point sources estimated from OMI. Geophysical Research Letters. 42(6), 1969-1976.

[41] Lu, Q., Zheng, J., Ye, S., Shen, X., Yuan, Z., and Yin, S. (2013). Emission trends and source characteristics of SO2, NOx, PM10 and VOCs in the Pearl River Delta region from 2000 to 2009. Atmospheric Environment. 76, 11-20.

[42] Lu, X., Yao, T., Li, Y., Fung, J. C., and Lau, A. K. (2016). Source apportionment and health effect of NOx over the Pearl River Delta region in southern China. Environmental Pollution. 212, 135-146.

[43] Buchholz, R. R., Paton-Walsh, C., Griffith, D. W., Kubistin, D., Caldow, C., Fisher, J. A., ... and Krummel, P. B. (2016). Source and meteorological influences on air quality (CO, CH4 & CO2) at a Southern Hemisphere urban site. Atmospheric Environment. 126, 274-289.

[44] Miller, M. B., Fine, R., Pierce, A. M., and Gustin, M. S. (2015). Identifying sources of ozone to three rural locations in Nevada, USA, using ancillary gas pollutants, aerosol chemistry, and mercury. Science of The Total Environment. 530, 483-492.

[45] Park, K., and Rhee, T. S. (2015). Source characterization of carbon monoxide and ozone over the Northwestern Pacific in summer 2012. Atmospheric Environment. 111, 151-160.

[46] Li, L., Chen, Z. M., Zhang, Y. H., Zhu, T., Li, S., Li, H. J., and Xu, B. Y. (2007). Heterogeneous oxidation of sulfur dioxide by ozone on the surface of sodium chloride and its mixtures with other components. Journal of Geophysical Research: Atmospheres. 112(D18).

Received: **21.02.2021**
Accepted: **19.03.2021**

CORRESPONDING AUTHOR

Xiansheng Liu
Joint Mass Spectrometry Center,
Cooperation Group Comprehensive Molecular Analytics,
Helmholtz Zentrum München,
German Research Center for Environmental Health,
Ingolstädter Landstr. 1,
85764 Neuherberg – Germany

e-mail: xiansheng.liu@helmholtz-muenchen.de